DMD Fast Forward. Published on February 7, 2006 as doi:10.1124/dmd.105.007732

Pimecrolimus: Absorption, Distribution, Metabolism, and Excretion in Healthy Volunteers Following a Single Oral Dose and Supplementary Investigations *In Vitro*

Markus Zollinger, Felix Waldmeier, Stefan Hartmann, Gerhard Zenke, Alfred G. Zimmerlin, Ulrike Glaenzel, Jean-Pierre Baldeck, Alain Schweitzer, Stephane Berthier, Thomas Moenius, and Maximilian A. Grassberger

Novartis Pharma AG, Basel, Switzerland (M.Z., F.W., S.H., A.G.Z., U.G., J.-P.B., A.S., S.B., T.M.) and Novartis Institutes for BioMedical Research, Basel, Switzerland (G.Z.) and Vienna, Austria (M.A.G.)

Running title:

Absorption and disposition of pimecrolimus in humans

Corresponding author:

Dr. Markus Zollinger

Novartis Pharma AG, WKL-135.2.21, P.O. box, CH-4002 Basel, Switzerland

Telephone: +41 61 696 45 24

Fax: +41 61 696 43 17

E-mail: markus.zollinger@novartis.com

Number of text pages:	36
Number of tables:	5
Number of figures:	7
Number of references:	24
Number of words in abstract:	234
Number of words in introduction:	540
Number of words in discussion:	1487

Abbreviations:

AUC, area under the concentration-time curve; P450, cytochrome P450; HPLC, high-pressure liquid chromatography; IL-2, interleukin-2; LC-MS, liquid chromatography-mass spectrometry; LSC, liquid scintillation counting; TFA, trifluoroacetic acid.

Abstract

The absorption and disposition of pimecrolimus, a calcineurin inhibitor developed for the treatment of inflammatory skin diseases, was investigated in four healthy volunteers following a single oral dose of 15 mg [^{3}H]pimecrolimus. Supplementary information was obtained from *in vitro* experiments. Pimecrolimus was rapidly absorbed. After t_{max} (1 - 3 h), its blood concentrations fell quickly to 3% of C_{max} at 24 h, followed by a slow terminal elimination phase (average $t_{1/2}$ 62 h). Radioactivity in blood decreased more slowly (8% of C_{max} at 24 h). The tissue- and blood cell distribution of pimecrolimus was high. The metabolism of pimecrolimus *in vivo*, which could be well reproduced *in vitro* (human liver microsomes), was highly complex and involved multiple oxidative *O*-demethylations and hydroxylations. In blood pimecrolimus was the major radiolabeled component up to 24 h (49% of radioactivity $AUC_{0\text{-}24\ h}$), accompanied by a large number of minor metabolites. The average fecal excretion of radioactivity between 0 and 240 h amounted to 78% of dose and represented predominantly a complex mixture of metabolites. In urine 0 - 240 h only about 2.5% of the dose and no parent drug was excreted. Hence, pimecrolimus was eliminated almost exclusively by oxidative metabolism. The biotransformation of pimecrolimus was largely catalyzed by CYP3A4/5. Metabolite pools generated *in vitro* showed low activity in a calcineurin-dependent T-cell activation assay. Hence, metabolites do not seem to contribute significantly to the pharmacological activity of pimecrolimus.

Pimecrolimus (SDZ ASM 981, Elidel®) is an ascomycin macrolactam that has been developed for the treatment of inflammatory skin diseases (Fig. 1). The compound inhibits calcineurin, a phosphatase that is essential for the translocation of the transcription factor NF-AT (nuclear factor of activated T-cells) into the cell nucleus. As a consequence, pimecrolimus inhibits the transcription and release of inflammatory cytokines and of other pro-inflammatory mediators in T-cells and mast cells (Grassberger et al., 1999). Pimecrolimus cream 1% is registered worldwide for the topical treatment of patients with mild to moderate atopic eczema (atopic dermatitis) and has been shown to be effective also in other inflammatory skin disorders such as allergic contact dermatitis and seborrheic dermatitis (Eichenfield and Beck, 2003; Wellington and Noble, 2004; Queille-Roussel et al., 2000; Rigopoulos et al., 2004). After topical administration, only low blood levels of pimecrolimus (typically below 1 ng/ml) were observed, even when large areas of affected skin were treated (Graham-Brown and Grassberger, 2003). Recently, pimecrolimus was shown to have therapeutic potential also after oral administration in patients with atopic eczema or psoriasis (Rappersberger et al., 2002; Wolff et al., 2003; Gottlieb et al., 2005). The pharmacokinetics of pimecrolimus after single and multiple oral administration has already been investigated in healthy subjects and patients with psoriasis, respectively (Scott et al., 2003). However, the disposition and metabolism of pimecrolimus in humans have not been reported, neither after topical nor after oral administration.

Here we report on the absorption, distribution, metabolism, and excretion of pimecrolimus in healthy volunteers after a single oral dose of 15 mg. Further, the metabolism of pimecrolimus *in vitro*, the identification of the responsible enzymes, and data on the pharmacological activity of the metabolites are presented. Information on the clearance processes, e.g. the responsible metabolizing enzyme, is key to predict and rationalize the pharmacokinetic drug-drug interaction potential. Knowledge about the pharmacological activity of metabolites may be important for

understanding the pharmacodynamics. In the case of pimecrolimus, these data are of relevance for the oral as well as for the topical administration of the compound as a cream. Due to the low systemic absorption of pimecrolimus after dermal administration only marginal blood levels and small amounts of metabolites in excreta are obtained which do not allow an appropriate investigation of the disposition after dermal application.

The oxidative metabolism of pimecrolimus is very complex, resulting in a plethora of minor metabolites, both in blood and excreta. All of them were present at low concentrations, were hardly separable by chromatography, and thus were hard to characterize in the sample matrices *ex vivo*. However, the same, very characteristic metabolite patterns were found in samples generated *in vitro*. The patterns resulted from oxidations by CYP3A at multiple positions of the pimecrolimus molecule, which appears to be a typical fate of bulky lipophilic CYP3A substrates. Thus it is not surprising that the *in vivo* patterns could be reproduced *in vitro* using hepatic microsomes. Therefore the analytically simpler *in vitro* samples were used for metabolite characterization, rather than the samples *ex vivo*. The same strategy had been used to compare the metabolism in humans and toxicological test species (Zollinger et al., 2002). The approach may be applicable to other developmental drugs when metabolism studies *in vivo* pose unsurmountable analytical difficulties.

Materials and Methods

Chemicals. NADPH, NADP, DL-isocitrate, and isocitrate dehydrogenase were obtained from Sigma (St. Louis, MO, USA), luciferin from Chemie Brunschwig (Basel, Switzerland), Rialuma™ liquid scintillation cocktail from Lumac (Groningen, The Netherlands), Pico-Fluor 40 and Permafluor E liquid scintillation cocktail from Packard (Meriden, CT, USA) and Titrisol® buffer concentrate from Merck (Darmstadt, Germany). All other reagents and solvents were of analytical grade and were readily available from commercial sources.

Study Drug. [^{3}H]Pimecrolimus was synthesized by the Isotope Laboratory of Novartis, Basel, Switzerland (Moenius et al., 2001). In the human *in vivo* study [^{3}H]pimecrolimus with the label in position 5 and 6 on the piperidine ring (see Fig. 1) and a specific radioactivity of 607 MBq/mmol was used. The radiochemical purity was >98%. The *in vitro* assays were performed with different batches of [^{3}H]pimecrolimus, again labeled in position 5 and 6. As an exception, the study on the distribution between blood cells and plasma was performed with [^{3}H]pimecrolimus labeled in position 32 on the cyclohexyl ring. Unlabeled pimecrolimus was a product of Novartis (Basel, Switzerland).

Subjects and Design of the Human *In Vivo* Study. The clinical part of the study was performed at Simbec Research Ltd. (Merthyr Tydfil, UK) in accordance with Good Clinical Practice guidelines and the Declaration of Helsinki (1964 and subsequent revisions). All subjects had to give written informed consent before participation. The protocol was approved by an institutional review board and ethics committee and by the Administration of Radioactive Substances Advisory Committee (ARSAC), UK.

Four healthy male subjects were enrolled in this open-label single oral dose absorption, distribution, metabolism, and excretion study. The subjects were of good health as shown by past medical history, physical examination, electrocardiogram, laboratory tests, and urine analysis.

Subjects of “poor metabolizer” genotype with regard to CYP2D6 were excluded (CYP2D6 was later found to be only marginally involved in the elimination of pimecrolimus). The subjects were non-smokers, had no history of alcoholism or drug abuse and did not take enzyme-inducing or -inhibiting drugs (e.g. phenobarbital, glutethimide, phenylbutazone, phenytoin, rifampin, isoniazid, dexamethasone, cimetidine, macrolides, ketoconazole, Ca-channel blockers) within four weeks prior to dosing. No medication other than the study drug was allowed from the initial day of screening (2 - 9 days before dosing) until the end of the evaluation period, with the exception of drugs needed to treat the subjects in the case of adverse events. The subjects had to fast for at least 10 h prior to dosing and to continue fasting for at least 4 h thereafter.

All subjects received a single oral 15 mg (11.2 MBq) dose of [^{3}H]pimecrolimus, formulated as a 20% solid dispersion containing, in addition, hydroxypropyl methyl cellulose (70%) and poloxamer 188 (10%). The dose was administered as three capsules of 5 mg [^{3}H]pimecrolimus, swallowed essentially simultaneously. The whole body radiation dose (“effective dose”) was calculated to be below the radiation dose limit for the public in the UK (0.5 mSv per year).

Blood was collected at 1, 2, 3, 4, 6, 8, 12, 24, 32, 48, 72, 96, 120, 144, 192, and 240 h postdose into EDTA-coated polypropylene tubes by direct venipuncture or by an indwelling cannula inserted in a forearm vein. Volumes of 25 ml were taken up to 120 h, followed by 5 ml samples at later times. Complete urine was collected in 24-h intervals between dosing and 240 h postdose. Each subject voided his bladder before drug administration and at the end of each collection interval. During a collection interval, the urine was kept refrigerated at 4 - 8°C. Complete feces were collected after dose administration up to 240 h postdose. The samples were stored at -20°C until analysis.

Radioactivity was measured in blood, urine, urine distillates, and feces by liquid scintillation counting (LSC). Concentrations of parent drug were determined in blood by liquid

chromatography-mass spectrometry (LC-MS). Metabolite patterns in blood, urine and feces were determined by high-pressure liquid chromatography (HPLC) with radioactivity monitoring following appropriate sample preparation. Details of the procedures are given below.

Safety assessments included the monitoring and recording of all adverse events, regular checks of routine blood chemistry, hematology and urine values, electrocardiogram recordings, measurements of vital signs and physical examinations.

Liquid Scintillation Counting of Human *In Vivo* Samples. Blood samples (duplicate 500 µl aliquots) were dried and combusted in a Canberra Packard (Schwadorf, Austria) model 307 sample oxidizer before LSC. Urine (duplicate 1 ml aliquots) and urine distillate samples (duplicate 300 µl aliquots of single distillates) were measured directly. Feces samples were homogenized in water. Aliquots of the homogenates (quadruplicate aliquots of approximately 0.7 g) were dried and combusted like the blood samples. The measurements in urine and urine distillates included volatile radioactivity (tritiated water); those in blood and feces did not because of drying. Pico-Fluor 40 and Permafluor E were used as liquid scintillation cocktails for the uncombusted and the combusted samples, respectively. The measurements were performed on a Wallac (Turku, Finland) 1409 liquid scintillation counter with counting times of 3 min (urine distillates) or 2 min (all other samples). Quench correction was performed by an external standard ratio method. To establish quench correction curves, sealed tritium standards (Packard) were used.

Determination of Parent Drug in Blood. Concentrations of pimecrolimus in individual blood samples were determined by LC-MS following extraction. The blood samples were diluted with two volumes of water before freezing in order to reduce the risk of coagulation. From each sample of diluted blood an aliquot of 1 ml was spiked with internal standard (21-propyl homolog of pimecrolimus; Novartis, Basel, Switzerland), alkalinized with 500 µl Titrisol® buffer

concentrate pH 10 and extracted with 5 ml of *tert*-butyl methyl ether (approximately 80% recovery). The organic extract was evaporated, re-constituted in 250 µl of water/methanol 20:80 (v/v) and 200 µl was injected. The chromatographic separation was performed at 75°C on a 250 x 4 mm Nucleosil 100 C18 AB column packed with 5 µm particles (Macherey-Nagel, Düren, Germany), preceded by an 8 x 4 mm precolumn of the same stationary phase. The components were eluted isocratically with 0.02 M aqueous ammonium acetate/methanol 15:85 (v/v) at a flow rate of 1 ml/min. Pimecrolimus (retention time about 4.4 min) and the internal standard (retention time about 5.2 min) were detected by mass spectrometry with negative ion atmospheric pressure chemical ionization and selected ion monitoring using an API 165 quadrupole mass spectrometer (PE Sciex, Foster City, CA, USA). The $[M-H]^-$ ions of pimecrolimus at m/z 808.6 and of the internal standard at m/z 822.6 were monitored. The limit of quantification was 0.11 pmol/ml (0.09 ng/ml), referring to undiluted blood.

Determination of Metabolite Patterns in Blood, Urine and Feces. Blood samples were partially hemolyzed by dilution with two volumes of water immediately after sampling. They were analyzed individually. Each sample of diluted blood was extracted three times with methanol. The extracts were acidified with trifluoroacetic acid (TFA) to a pH of about 3.5 (pimecrolimus solutions are most stable at pH 2 - 3; unpublished data), combined and evaporated to dryness. The residue was re-constituted in three different solvents in the following way: first it was taken up in water/methanol 80:20 (v/v) by sonication, followed by centrifugation and separation of the supernatant (extract A). The remaining pellet was extracted two more times, once with water/methanol 60:40 (v/v) containing 0.012% (v/v) TFA (extract B), once with water/acetonitrile 40:60 (v/v) containing 0.008% (v/v) TFA (extract C). The three extracts were analyzed in a single HPLC run after sequentially loading them onto the column in the order

DMD Fast Forward. Published on February 7, 2006 as DOI: 10.1124/dmd.105.007732
This article has not been copyedited and formatted. The final version may differ from this version.

C-B-A. By this procedure, both polar and non-polar components were dissolved and concentrated on the head of the HPLC column before starting the elution.

Urine was pooled over the collection interval of 0 to 168 h for each subject individually. Of each pool, 2.7 ml was diluted with 0.3 ml acetonitrile and acidified with TFA to a pH of about 3. After centrifugation, an aliquot of the supernatant was injected onto the HPLC column. The contributions of tritiated water to the radioactivity in the urine pools were determined by measuring radioactivity in native and dried aliquots.

Feces homogenates were pooled over the collection interval of 0 to 168 h for each subject individually and the samples were processed as described above for blood.

The recovery of radioactivity after sample processing and HPLC was around 100% for blood and urine. For feces, the recovery of radioactivity was 74 - 83% after sample preparation and about 91% (of the amount injected onto the column) after HPLC. The stability of pimecrolimus during blood and feces sample processing and HPLC analysis was investigated using blank samples spiked with [^{3}H]pimecrolimus. No degradation of pimecrolimus was detected. The stability of the numerous metabolites in blood and feces during sample processing and HPLC was not investigated. However, due to their structural similarity to the parent drug (mainly products of *O*-demethylations, hydroxylations and oxidative dechlorination with intact macrocycle; see below) they can be assumed to be stable as well.

The chromatography was performed on an HP 1090 liquid chromatograph (Hewlett-Packard, Waldbronn, Germany). Radioactivity was monitored by LSC either off-line after collection of 0.5 min fractions (blood extracts and urine samples) or on-line using a Berthold (Wildbad, Germany) LB 507A radioactivity monitor. For the latter purpose 3 ml/min of Rialuma^{TM} liquid scintillation cocktail was added to the column effluent. The separations were performed on a 250 x 4.6 mm Nucleosil 100 C18 AB column (5 µm particles), preceded by an 8 x 4 mm

precolumn of the same stationary phase. The column temperature was 60°C. The components were eluted with a gradient of 0.02% (v/v) aqueous TFA (mobile phase A) *versus* acetonitrile (mobile phase B). The proportion of the mobile phase B was kept at 10% till 5 min after injection and was then increased linearly to 100% at 140 min where it was kept for another 10 min. The total flow rate was 1 ml/min.

Blood concentrations and percentages of dose in the excreta were estimated for pimecrolimus and its metabolites from the radiochromatograms based on the relative peak areas and the concentrations or amounts of radioactivity in the original biological samples, following subtraction of the losses during sample preparation and chromatography.

Pharmacokinetic Calculations. Pharmacokinetic parameters *in vivo* were calculated using non-compartmental methods. They are given as mean ± S.D. except for t_{max} for which medians are given. Area under the concentration-time curve- (AUC-) values were calculated by the linear trapezoidal method and extrapolated to infinity according to $AUC_{t-\infty} = C_t \cdot t_{1/2} / \ln 2$. The $t_{1/2}$ values were calculated by log-linear regression of plasma concentrations during the terminal elimination phase.

The amount of total tritiated water formed in the body was estimated from the radioactivity concentrations in the distillates of the urine samples collected between 72 and 240 h postdose. The concentrations were extrapolated back to time zero assuming a half-life of 9.5 days (Richmond et al., 1962). The extrapolated concentrations were multiplied by the amounts of total body water, taken as 55% of the individual body weights (Richmond et al., 1962) to obtain the total amounts of tritiated water formed, which were expressed as percent of dose.

Distribution of Pimecrolimus Between Blood Cells and Plasma *In Vitro*. Pooled fresh heparinized blood from three human donors was spiked with [^{3}H]pimecrolimus at five concentrations in the range of 1 ng/ml to 1 µg/ml and incubated in triplicates at 37°C for 30 min.

Thereafter, two aliquots were removed and the remaining blood was centrifuged to obtain plasma. Radioactivity concentrations in all whole blood- and plasma samples were determined by LSC. The stability of [^{3}H]pimecrolimus during the incubation was confirmed by HPLC analysis with radioactivity monitoring of blood extracts. No degradation was found during 1.5 h at 37°C.

Metabolism of [^{3}H]Pimecrolimus by Human Liver Microsomes. A commercial pool of liver microsomes from ten individuals (Gentest, Woburn, MA, USA; Catalog No. H161, Lot No. 7) with a total cytochrome P450 (P450) content of 0.42 nmol/mg protein was used. Microsomal incubations were performed at 37°C in 0.1 M phosphate buffer pH 7.4, containing 0.2 mM NADPH and an NADPH regenerating system consisting of (final concentrations) 1 mM NADP, 5 mM DL-isocitrate, 1 U/ml isocitrate dehydrogenase and 5 mM $MgCl_2$. [^{3}H]Pimecrolimus was added as a solution in acetonitrile. The concentration of acetonitrile in the final incubate was less or equal 0.7% (v/v). [^{3}H]Pimecrolimus was incubated at 1 µM initial substrate concentration with 50 µg microsomal protein/ml or at 40 µM initial substrate concentration with 4 mg microsomal protein/ml for different times. In all incubates the concentration of radioactivity was 0.22 MBq/ml. The enzymatic reactions were stopped by adding one volume of ice-cooled acetonitrile, followed by cooling on ice for 5 min and ultracentrifugation. Aliquots of the supernatants of the 1 and 40 µM [^{3}H]pimecrolimus incubates were analyzed by HPLC with radioactivity detection using the chromatographic conditions described above for the *in vivo* samples. Moreover, aliquots of the 40 µM [^{3}H]pimecrolimus incubates were investigated by LC-MS with parallel radioactivity monitoring as described below for characterizing metabolite structures. The chemical stability of [^{3}H]pimecrolimus (1 µM) under the incubation conditions was checked by a control incubation for 120 min (longest incubation time used in the study) in the absence of microsomes. The degradation amounted to less than 2%.

DMD Fast Forward. Published on February 7, 2006 as DOI: 10.1124/dmd.105.007732
This article has not been copyedited and formatted. The final version may differ from this version.

Structural Characterization of *In Vitro* Metabolites by LC-MS. The chromatographic part of the instrumentation consisted of two Kontron (Milan, Italy) 420 pumps, a manual Rheodyne (Cotati, CA, USA) 7725i injector and an SPH 99 column oven from Spark Holland (Emmen, The Netherlands). After the column, the flow was split into two parts. Between 70 and 95% of the flow was combined with Rialuma^{TM} (3 ml/min) and directed into a Berthold LB 507B radioactivity monitor. The remaining 5 - 30% of the effluent was passed into the electrospray LC-MS interface (model API 2, Finnigan MAT, San Jose, CA, USA) of a Finnigan MAT TSQ7000 tandem quadrupole mass spectrometer. The HPLC column, the column temperature, the mobile phase gradient and the total flow rate were the same as described above in the context of the metabolite patterns *in vivo*. In front of the electrospray interface a flow of 1 µl/min of aqueous 50 mM lithium acetate was added by a syringe pump to generate $M+Li^+$ ions. The electrospray interface was operated with nitrogen as sheath gas (80 psi), nitrogen as auxiliary gas (10 flowmeter units) and methanol/water 90:10 (v/v) as sheath liquid (20 µl/min). The spray capillary was set to 4.5 kV. The transfer capillary was heated to 290 - 350°C. Single-stage positive ion mass spectra were taken at unit mass resolution by using the first quadrupole as mass analyzer. The range of m/z 200 - 1100 was scanned in 2 s. The upfront collision offset was set to 0 V. Thermal excitation in the heated capillary of the LC-MS interface was sufficient to generate fragment ions.

For determining the number of exchangeable hydrogens of the metabolites, LC-MS runs were performed as described above except that D_2O was used instead of H_2O in the mobile phase A and as solvent for lithium acetate. No sheath liquid was used in these experiments.

***In Vitro* Characterization of Isoenzymes Responsible for Pimecrolimus Metabolism; Enzyme Kinetics.** Microsomes prepared from recombinant human B-lymphoblastoid cell lines heterologously expressing human P450 isoenzymes (CYP1A2, CYP2A6, CYP2B6, CYP2C8,

CYP2C9, CYP2C19, CYP2D6, CYP2E1, CYP3A4, and CYP4A11) or expressing P450 reductase only (control) were obtained from Gentest. [^{3}H]Pimecrolimus was incubated with these microsomes for 20 min at an initial substrate concentration of 1 µM under conditions recommended by the supplier. The incubation volumes were 200 µl. The amount of recombinant P450 added (12.5, 21.5, 5.3, 19.4, 13.5, 12.3, 6.4, 8.3, 29.1, and 17.0 pmol of CYP1A2, CYP2A6, CYP2B6, CYP2C8, CYP2C9, CYP2C19, CYP2D6, CYP2E1, CYP3A4, and CYP4A11, respectively) was representative of either the highest P450 concentration or the highest P450 marker activity found for the respective isoform in a panel of 12 individual human liver microsomes (Gentest, Catalog No. H003, H006, H023, H030, H042, H043, H056, H066, H070, H089, H093, and H112).

For determining enzyme kinetic parameters (K_m, V_{max}) as well as for investigating the effect of the CYP3A inhibitor ketoconazole or of a specific anti-CYP3A4/5 monoclonal antibody (Gentest, Catalog No. A334, Lot No. 2) on the metabolism of [^{3}H]pimecrolimus, the compound was incubated for 10 min with pooled human liver microsomes from six individual donors (Gentest, Catalog No. H161, Lot No. 3) at 0.1 mg/ml microsomal protein. The extent of biotransformation of [^{3}H]pimecrolimus was shown before to increase linearly with incubation time and microsomal protein concentration up to 15 min and 0.5 mg/ml, respectively. For investigating the enzyme kinetics, initial substrate concentrations of 0.1 - 8 µM were used. For the inhibition experiments initial substrate concentrations of 1 µM were chosen. The ketoconazole concentrations were between 0.1 and 2 µM. For the antibody inhibition experiments, human liver microsomes (pool of six individuals) were pre-treated with increasing amounts of monoclonal antibody according to the recommendations of the supplier (Gentest). Immuno-inhibited human liver microsomes were incubated at a final human liver microsomal

DMD Fast Forward. Published on February 7, 2006 as DOI: 10.1124/dmd.105.007732
This article has not been copyedited and formatted. The final version may differ from this version.

protein concentration of 0.1 mg/ml for 10 min with either 1 µM [^{3}H]pimecrolimus or 50 µM midazolam.

All enzymatic reactions were stopped by the addition of ice-cooled acetonitrile, followed by centrifugation. The supernatants were analyzed by HPLC with radioactivity monitoring to determine the rate of disappearance of [^{3}H]pimecrolimus or with UV detection to determine the rate of formation of hydroxy-midazolam.

Determination of Pharmacological Activity of Metabolite Pools by Interleukin-2 Reporter Gene Assay. [^{3}H]Pimecrolimus (10 µM initial concentration; 0.22 MBq/ml) was incubated with human liver microsomes (1 mg microsomal protein/ml) for 5, 15 or 60 min. The microsomes and the concentrations of NADPH and of the components of the NADPH regenerating system were the same as described above for the *in vitro* metabolism investigations. Two pools of metabolites were isolated from each of the three incubates by preparative HPLC: a metabolite Fraction 1 (highly polar metabolites) eluting between 0 and approximately 10 min and a metabolite Fraction 2 (moderately polar and nonpolar metabolites but no parent drug) eluting between approximately 10 and 93 min under the chromatographic conditions of the metabolite patterns (cf. *Results* section). Fractions 1 and 2 were evaporated and re-dissolved in water (Fractions 1) or water/ethanol 1:1 (v/v) (Fractions 2). The amounts of total [^{3}H]pimecrolimus metabolites in the isolated fractions were determined from the total radioactivity, measured by LSC, and the specific radioactivity of the parent drug in the microsomal incubates. Small aliquots of Fractions 2 were analyzed by HPLC to confirm the metabolite patterns and the absence of unchanged [^{3}H]pimecrolimus (except for insignificant traces).

For determining the effects of the solvents and of pimecrolimus-unrelated components from the incubation medium on the interleukin-2 (IL-2) reporter gene assay, incubations of human liver microsomes without pimecrolimus were performed, which were processed identically to the

pimecrolimus incubates described above. Fraction 1 and Faction 2 samples of the control incubates did not show any significant activity in the IL-2 reporter gene assay at dilutions of ≥1:50 and ≥1:200, respectively (data not shown). Furthermore, when these samples were spiked with 1 nM pimecrolimus, the pimecrolimus activity was not affected at dilutions of ≥1:50 of Fraction 1 and ≥1:500 of Fraction 2 (data not shown). Thus, the Fraction 1 and Fraction 2 samples containing pimecrolimus metabolite pools were diluted at least 1:50 and 1:500, respectively.

The IL-2 reporter gene assay was performed as described previously (Zenke et al., 2001). Briefly, the luciferase gene was placed under the transcriptional control of the human IL-2 promoter and stably transfected into the human T-cell line Jurkat. IL-2 promoter-driven luciferase expression was quantified by measuring the bioluminescence upon reaction with its substrate luciferin. Its production correlated with IL-2 expression and was thus a direct measure of IL-2 transcription. Cells were stimulated with 20 ng/ml phorbol myristate acetate and 1 µg/ml phytohemagglutinin in the presence of serial dilutions of test samples in duplicates and incubated 5.5 h at 37˚C. Serial dilutions (0.01 - 10 nM in duplicates) of unlabeled pimecrolimus (1 mM stock solution in ethanol) were performed on each assay plate and the resulting dose-response curves were used to quantify the pimecrolimus-related pharmacological activity of the test samples. In two independent experiments, serial dilutions of the pimecrolimus metabolite pools were tested. The IC_{50} values of pimecrolimus were between 0.6 and 1.0 nM. Pimecrolimus did not show any activity at 0.12 - 0.37 nM concentrations.

DMD Fast Forward. Published on February 7, 2006 as DOI: 10.1124/dmd.105.007732
This article has not been copyedited and formatted. The final version may differ from this version.

Results

Demographic, Safety and Tolerability Data from Human *In Vivo* Study. Four healthy, male Caucasian subjects were enrolled and completed the study. The subjects were of a mean age of 38 years (range 37 - 41 years), of a height of 176 ± 11 cm (mean ± S.D.; range 163 - 189 cm) and weighed 80.4 ± 13.7 kg (mean ± S.D.; range 67.5 - 99.4 kg; within ±15% of normal for height and frame size). Pimecrolimus was well tolerated without serious adverse events or discontinuation due to an adverse event. No drug-related adverse events or clinically significant changes in vital signs, clinical chemistry, or electrocardiographic parameters were observed. No concomitant medication due to an adverse event was required.

Blood Concentrations of Radioactivity and Pimecrolimus; Pharmacokinetic Parameters *In Vivo*. Both the total radiolabeled components (radioactivity) and pimecrolimus reached their maximum blood concentrations already at 1 h (median value) following the oral dose of 15 mg [^{3}H]pimecrolimus. After t_{max}, the average blood concentrations of pimecrolimus decreased rapidly to 11% of C_{max} at 8 h and 3% at 24 h. The average blood concentrations of radioactivity decreased more slowly to 8% of C_{max} at 24 h (Fig. 2, Table 1). The terminal half-life of radioactivity in blood could only roughly be estimated (approximately 145 h) and was clearly longer than that of the parent drug (62 h on average). The $AUC_{0-\infty}$ of radioactivity in blood was approximately four times higher than that of the parent drug.

Metabolite Patterns in Blood, Urine and Feces. Metabolite patterns in blood could be analyzed up to 24 h postdose (examples in Fig. 3A and B). The radiochromatograms showed a double peak for pimecrolimus (stable tautomers), a large number of very minor and only partially separated metabolites of moderate or low polarity (50-95 min retention time) and a front-peak. Except for the front-peak, metabolite Dx_1 (for metabolite nomenclature see below) was the most prominent biodegradation product in blood and the only one that could be observed

consistently in most of the blood radiochromatograms. Its retention time coincided with that of the major primary metabolite of pimecrolimus in human liver microsomal incubates (see below), suggesting that the *in vivo* and *in vitro* metabolite was identical. This was supported by data in the rat as detailed below in the context of the *in vitro* metabolism of pimecrolimus. The parent drug was the most abundant radiolabeled component in human blood up to 24 h, contributing about half of the $AUC_{0\text{-}24\ h}$ of total radioactivity (Table 2). The metabolites of moderate to low polarity showed their highest blood concentrations around 1 to 3 h and disappeared thereafter approximately in parallel with the parent drug. In contrast to other peaks in the radiochromatograms, the front-peak tended to increase with time, both in terms of relative and absolute abundance, at least up to 24 h. The highly polar metabolite(s) constituting this peak may have contributed significantly to the radioactivity in the blood after 24 h, though being present at very low concentrations only.

The small amounts of radioactivity excreted in urine (2.3 ± 0.5% of dose between 0 and 168 h; mean ± S.D.) consisted mainly of highly polar, chromatographically unretained material, a minor part of which (0.5 ± 0.2% of dose in urine collected between 0 and 168 h) was due to tritiated water (example of a radiochromatogram in Fig. 3C). No parent drug was detected in urine.

The metabolite patterns in feces were extremely complex, consisting mainly of a very broad and complex peak of unresolved metabolites centered at 55 min but extending from 20 to 90 min retention time (example in Fig. 3D). Minor amounts of parent drug were observed in the feces of three of the four subjects and minor front-peaks were found in the feces chromatograms of all four subjects.

Only 0.8 ± 0.5% of the administered radioactivity (mean ± S.D.) was converted to tritiated water in total. The low extent of tritiated water formation demonstrated that the ^{3}H-label was placed in a metabolically stable position.

Due to the low amounts of pimecrolimus metabolites in blood and urine and the complexity of the radiochromatograms of the feces extracts, no attempt was made to directly characterize the structures of the metabolites *in vivo*. Instead, material from incubates of [^{3}H]pimecrolimus with human liver microsomes was used to obtain structural information on the biotransformation products (see paragraph on metabolite structures).

Excretion of Radioactivity in Urine and Feces. Radioactivity was excreted predominantly with the feces (78 ± 14% of dose between 0 and 240 h; mean ± S.D.). Only 2.5 ± 0.6% of the administered radioactivity appeared in urine between 0 and 240 h (Table 3). Most of the excretion occurred between 0 and 96 h postdose (on average 72% of dose in feces, 2.0% in urine). The recovery of radioactivity up to 240 h varied considerably between the subjects, ranging from 63 to 94% of dose. The reason for the low recovery, mainly in one subject, remains unknown but may be due to losses during feces collection.

Blood Distribution of Pimecrolimus *In Vitro*. The distribution of pimecrolimus between human plasma and blood cells *in vitro* was found to be concentration-dependent (Table 4). At low blood concentrations (≤ 34 ng/ml) only approximately 12% of the compound was localized in plasma. At higher concentrations the percentage in plasma increased up to approximately 70% at 1 µg/ml.

Metabolite Patterns in Incubates of [^{3}H]Pimecrolimus with Human Liver Microsomes. The biotransformation of pimecrolimus was further investigated *in vitro* using human liver microsomes. At 1 µM initial substrate concentration and a concentration of microsomal protein of 50 µg/ml, the metabolite patterns shown in Fig. 3E-H were obtained. The patterns after short incubation times (5-10 min) closely resembled those obtained in blood *in vivo* between 1 and 8 h postdose. With increasing incubation times, the complexity of the patterns and the average polarity of the metabolites gradually increased until patterns like those in the feces (Fig. 3D) were

obtained. Hence, metabolite patterns very similar to those found *in vivo* could be generated *in vitro*. Therefore, the structural characterization of metabolites was limited to those formed *in vitro*, which were much better amenable to LC-MS analysis than those in the *in vivo* samples due to higher concentrations and a less complex background of drug-unrelated components. The similarity of the metabolism of pimecrolimus *in vitro* and *in vivo* was further supported by data from the rat (not shown) which metabolized pimecrolimus by similar pathways as humans. Following an oral dose of 100 mg/kg pimecrolimus, major metabolites (including Dx_1) in rat blood could be characterized mass spectrometrically and compared in detail with those formed by rat liver microsomes. The data showed a close correspondence of the *in vivo* and *in vitro* metabolism.

In order to obtain sufficient amounts of metabolites for LC-MS analysis, [^{3}H]pimecrolimus was incubated additionally at an initial substrate concentration of 40 µM and with 4 mg microsomal protein/ml for 2 and 60 min. The metabolite patterns were almost identical with those obtained at 1 µM initial substrate concentration and 50 µg microsomal protein/ml, suggesting that both qualitatively and quantitatively the same metabolites were formed under the two incubation conditions despite potential enzyme saturation at 40 µM substrate concentration.

Metabolite Structures. The chemical structures of pimecrolimus metabolites formed in human liver microsomal incubations (described above) were investigated by LC-MS with electrospray ionization in the positive ion mode. Lithium acetate was added post-column in order to form $M+Li^+$ ions. In the absence of lithium acetate, pimecrolimus formed a mixture of adduct ions, including $M+Na^+$, while essentially no $M+H^+$ ions were observed (data not shown). The mass spectrum of pimecrolimus itself (Fig. 4) showed the $M+Li^+$ ion at m/z 816 together with a number of fragment ions of which Fragment A, resulting from a cleavage of the macrocyclic ring at the C24,C25-bond and the O,C26-bond, predominated. The cleavages were induced by thermal

activation in the heated capillary between the ion source and the mass analyzer. Very similar fragmentations were obtained by the more conventional collisional activation method (data not shown). Metabolites of pimecrolimus also formed $M+Li^+$ and Fragment A-type ions, which allowed to localize metabolic changes within Fragment A (substructure x) or outside Fragment A (substructure y, cf. Fig. 4). Cleavage products in addition to Fragment A were observed in a few of the mass spectra of the metabolites. They were in agreement with the proposed partial structures described below. Further support of these structures was obtained by mass spectrometric H/D exchange experiments which revealed the number of heteroatom-bound hydrogens.

The results of the mass spectrometric characterization of the metabolites in a 2 min incubate of [^{3}H]pimecrolimus with human liver microsomes is shown in Fig. 5 in the form of a radiochromatogram labeled with metabolite names which reflect the type and number of metabolic changes. The legend of Fig. 5 explains the nomenclature.

Clearly the main type of biotransformation was (oxidative) *O*-demethylation (reaction code D), which can occur at positions 13, 15 or 31. The major primary metabolite, Dx_1, which was observed also in blood *in vivo* (see above), had undergone demethylation at position 13 or 15. These two remaining possibilities could not be distinguished on the basis of the available mass spectrometric data. As additional biotransformations, hydroxylations (reaction code O) and oxidative dechlorination (reaction code K), resulting in a keto group at position 32, were observed. The elution order of the metabolites was consistent with the proposed biotransformations in the sense of a decrease in retention time for each additional polar group generated.

The mass spectral data on the metabolites in the 60 min incubate with human liver microsomes (data not shown) suggested that the further biodegradation products formed at this

longer incubation time were simply products of consecutive biotransformations of the types found already in the 2 min incubate. Additional types of metabolic reactions were of negligible importance. The observed biotransformations, including possible tautomerizations (see *Discussion*), are summarized in Fig. 6.

Enzyme Kinetics and P450 Isoforms Responsible for Pimecrolimus Metabolism in Humans. The rate of metabolism of pimecrolimus by human liver microsomes followed apparent single-enzyme Michaelis-Menten kinetics with K_m and V_{max} values of 0.7 µM and 394 (pmol/min)/mg protein, respectively. From a panel of ten P450 isoenzymes tested, CYP3A4 dominated against all other isoforms with regard to the turnover of [^{3}H]pimecrolimus under the experimental conditions used (Fig. 7). CYP2A6, CYP2C19, CYP2D6, and CYP2E1 also metabolized pimecrolimus, though at a relatively low rate, while no measurable biotransformation occurred with CYP1A2, CYP2B6, CYP2C8, CYP2C9, and CYP4A11. In line with this result, ketoconazole, a well established high-affinity inhibitor probe against CYP3A isoforms *in vitro* (Baldwin et al., 1995), strongly inhibited the metabolism of pimecrolimus (1 µM) by human liver microsomes with an IC_{50} of 0.25 µM. Moreover, a monoclonal antibody inhibitory to CYP3A4/5 inhibited the metabolism of pimecrolimus (1 µM) and the hydroxylation of midazolam (mediated predominantly by CYP3A4/5; Kronbach et al., 1989) to a similar extent. These data suggest that CYP3A4 and possibly CYP3A5 play a major role in the biotransformation of pimecrolimus in humans.

Pharmacological Activity of Metabolites. Pools of metabolites of pimecrolimus, isolated from incubates with human liver microsomes, were investigated for immunosuppressive activity using an IL-2 reporter gene assay. To cover the full range of biodegradation products, microsomal incubations were performed for 5, 15 and 60 min. The metabolite pattern in the 5 min incubate resembled that in Fig. 3E (and that in blood in Fig. 3A), that in the 15 min

incubate resembled the pattern in Fig. 3G and that in the 60 min incubate resembled the pattern in Fig. 3H, though without any parent drug left. The metabolites in the three incubates were isolated by HPLC in the form of two pools. Fraction 1 contained only highly polar metabolites (corresponding to those eluting between 0 and about 10 min in Fig. 3); Fraction 2 contained the moderately polar and nonpolar metabolites (corresponding to those eluting between about 10 and 93 min in Fig. 3), but no parent drug.

The Fractions 1 were devoid of immunosuppressive activity. The Fractions 2 showed moderate to low activities, decreasing with increasing incubation time, i.e. with increasing polarity of the metabolites (Table 5). The highest concentration-normalized activity was found in Fraction 2 of the 5 min incubate, amounting to 9% of the concentration-normalized activity of pimecrolimus.

Discussion

In the present study, the absorption and disposition of pimecrolimus were investigated in healthy volunteers after a single oral dose of 15 mg. Supplementary information on the blood distribution, the biotransformation, including a characterization of the responsible enzymes, as well as on the pharmacological activity of the metabolites was obtained from *in vitro* investigations.

Pimecrolimus was rapidly absorbed. Maximum blood concentrations of radioactivity and parent drug were reached at 1 h after dosing in three subjects and at 2 to 3 h in one subject. The small amounts of parent drug detected in feces (0.7 ± 0.9 of dose) suggest a nearly complete absorption. Even though some of the unabsorbed pimecrolimus may have undergone degradation by the intestinal microflora, this does not seem to be a significant process. Metabolism by intestinal microorganisms is expected to occur predominantly by reduction and hydrolysis (Scheline, 1973; Smith, 1978) while under *in vitro* conditions producing very similar metabolite patterns as in feces (Fig. 3), only products of oxidative biotransformation were identified. The absolute oral bioavailability of pimecrolimus could not be determined from the data of the present study.

At t_{max} of radioactivity, pimecrolimus accounted for about 70% of the radioactivity in blood. Thereafter, the parent drug concentrations decreased rapidly and faster than those of the radioactivity, reflecting the increasing presence of metabolites in the circulation, predominantly highly polar ones. The terminal half-lives of parent drug (average $t_{1/2}$ 62 h) and radioactivity ($t_{1/2}$ approximately 145 h) in blood were rather long.

The extent of tissue distribution of pimecrolimus was probably high as the terminal volume of distribution divided by the bioavailability amounted to 6700 liters, on average. Within the blood compartment, the distribution of pimecrolimus between blood cells and plasma was

concentration-dependent (*in vitro* data). At the blood concentrations found after a 15 mg oral dose, the compound resided predominantly in the blood cells (approximately 12% in plasma). However, at higher blood concentrations the fraction in plasma increased.

The metabolism of pimecrolimus, both *in vivo* and *in vitro*, was found to be highly complex due to numerous parallel and consecutive biotransformations. The occurrence of multiple relatively stable tautomers of the metabolites further increased the complexity of the chromatograms (see below). The complexity was most obvious from the metabolite patterns in feces, showing a broad peak of chromatographically unresolved components. However, also in blood the number of metabolites (all minor) was too high for complete chromatographic separation. Therefore, no attempt was made to directly determine the structures of the metabolites *in vivo*. Instead, *in vitro* metabolites, formed in incubates with human liver microsomes, were investigated. The substitution of *in vitro* for *in vivo* metabolites for structural characterization is justified both by the similarity of the metabolite patterns in the two human systems (Fig. 3) and by an *in vitro - in vivo* comparison of the pimecrolimus metabolism in the rat based on retention times as well as mass spectra, as mentioned in the *Results* section..

For a large number of *in vitro* metabolites LC-MS provided structural information (mainly partial structures) and hence information on the types and number of metabolic reactions. The metabolites of the first-generation formed by human liver microsomes were mainly products of (oxidative) *O*-demethylations, including the most abundant metabolite Dx_1 which had undergone *O*-demethylation at position 13 or 15. The two possibilities could not be differentiated. It is notable that four metabolites with code Dx (Dx_1, Dx_2, Dx_3, and Dx_5), which had undergone a single *O*-demethylation in substructure x (see Fig. 4 and legend of Fig. 5), were detected even though there are only two *O*-methyl groups in this substructure. This can be explained with the existence of relatively stable, slowly interconverting tautomers, appearing as

separate chromatographic peaks, as observed for the parent drug. The phenomenon of stable tautomers has been described before for structurally related macrolides (Hughes et al., 1992; Namiki et al., 1993). Demethylations in substructure x generate hydroxy groups capable of forming additional hemiacetal functions with the tricarbonyl system, thereby increasing the number of possible tautomers, compared with those of pimecrolimus. In contrast, only one product of an *O*-demethylation in substructure y (Dy_6; demethylated at position 31) was observed. As additional metabolic reactions, hydroxylations and, to a minor extent, oxidative dechlorination were observed. Second- and higher generation metabolites appeared to be formed mainly by consecutive *O*-demethylations and hydroxylations. Interestingly, no products of an opening of the macrocycle were found among the metabolites characterized by LC-MS. Even though a lactone hydrolysis might have been followed by a dehydration, resulting in a zero net change in molecular weight, such a sequence of biotransformations would have resulted in an additional exchangeable hydrogen, which would have been noted by mass spectrometric H/D exchange experiments. This is in contrast to the behavior of the related macrolides rapamycin and SDZ RAD 001 which undergo prominent cleavage at the lactone group (Vidal et al., 1998; Streit et al., 1996). The front peak, observed both in the *in vitro* and *in vivo* metabolite patterns, seems to be due to one or several highly polar metabolites of pimecrolimus which, because of their polarity, appear to contain only a small structural fragment of the parent drug molecule, including the labeled piperidine ring. Even though these components might have accounted for a considerable portion of the radioactivity in blood at late times after dosing, their quantitative importance, expressed in percent of dose, was small (less than 4%), as judged from the metabolite patterns in the excreta.

The very small amounts of unchanged parent drug observed in the excreta (0.7% of dose on average) suggest that pimecrolimus is eliminated from the human body predominantly by

oxidative metabolism. Even if biliary excretion of unchanged pimecrolimus, followed by degradation in the intestinal lumen, cannot be excluded, it seems unlikely that this was a major process, as discussed above in the context of absorption. Moreover, bile of rats treated intravenously with [^{3}H]pimecrolimus did not contain any unchanged parent drug (data not shown). In the human subjects, radiolabeled material was excreted almost exclusively *via* the feces, indicating a predominance of biliary over renal excretion of pimecrolimus metabolites. A direct secretion of pimecrolimus metabolites through the intestinal wall into the intestinal lumen, as an alternative to biliary excretion, cannot be excluded but seems unlikely as in bile duct cannulated rats treated intravenously with [^{3}H]pimecrolimus, 93% of the administered radioactivity was excreted in the bile while only 2.4% appeared in the feces (data not shown).

The oxidative steps of pimecrolimus biotransformation are likely to be catalyzed by cytochrome P450 enzymes. Incubations with a panel of heterologously expressed single P450 isoenzymes and experiments with P450 isoenzyme-specific inhibitors revealed that CYP3A4/5 is mainly responsible for the metabolism of pimecrolimus. The broad catalytic selectivity of CYP3A4 (Guengerich, 1999) and its ability to oxidize substrates in multiple positions (Smith and Jones, 1992) may at least partially explain the complexity of the metabolism of pimecrolimus. In addition to CYP3A4/5, a few other P450 isoforms were shown to be able to metabolize [^{3}H]pimecrolimus to some extent. The increase in exposure that an inhibition of the CYP3A pathway *in vivo* may provoke is therefore likely to be limited by the existence of alternative enzymes capable of metabolizing pimecrolimus. As the metabolism of pimecrolimus by CYP3A5 was not specifically investigated, its contribution, relative to that of CYP3A4, remains unknown.

The pharmacological activity of metabolite pools was assessed by an IL-2 reporter gene assay, a very sensitive *in vitro* test that is relevant for the principal mode of action of pimecrolimus. Using this assay, only low activity was observed with pools of moderately polar to nonpolar

metabolites, whereas pools of highly polar metabolites (front peaks) showed no measurable activity at all. The biotransformation of pimecrolimus thus appears to be associated, in general, with a loss of pharmacological activity, an effect which increases with the degree of hydrophilicity of the metabolites. Therefore, and because of their low blood concentrations, the metabolites may contribute only to a small extent, if at all, to the therapeutic effect of orally administered pimecrolimus in patients with inflammatory skin diseases.

In conclusion, pimecrolimus is rapidly absorbed in fasting humans following a single oral dose of 15 mg. After t_{max}, the blood concentrations of pimecrolimus decrease rapidly, followed by a long terminal elimination phase. The compound seems to be extensively distributed into tissues. Its distribution into blood cells is high and concentration-dependent. Numerous parallel and consecutive biotransformations, together with the occurrence of multiple relatively stable tautomers, leads to complex metabolite patterns in blood and feces which could be reproduced in incubates with human liver microsomes. The main metabolic pathways are *O*-demethylations. CYP3A4 and possibly CYP3A5 provide the most important contribution(s) to the biotransformation of pimecrolimus. The elimination of pimecrolimus occurs almost exclusively by oxidative metabolism. The metabolites are excreted mainly *via* the bile into the feces. In urine little drug-related material and no unchanged pimecrolimus is excreted. The metabolites are unlikely to contribute significantly to the pharmacological activity of the compound.

Acknowledgments. The authors would like to thank Dr. Jeffrey T. Smith from Simbec Research Ltd. (Principal Investigator), Dr. Pascale Burtin (Clinical Pharmacology Physician) and Dr. Jean-Baptiste Lecaillon (Bioanalytics and Pharmacokinetics Scientist) for their support of the human absorption, distribution, metabolism, and excretion study. The work by Mr. Bertrand Birlinger (*in vitro* enzyme identification), Mrs. Regina Klünder (*in vitro* blood distribution) and Mrs. Ulrike Strittmatter (IL-2 reporter gene assay) is gratefully acknowledged.

References

Baldwin SJ, Bloomer JC, Smith GJ, Ayrton AD, Clarke SE, and Chenery RJ (1995) Ketoconazole and sulphaphenazole as the respective selective inhibitors of P4503A and 2C9. *Xenobiotica* **25:**261-270.

Eichenfield LF and Beck L (2003) Elidel (pimecrolimus) cream 1%: a nonsteroidal topical agent for the treatment of atopic dermatitis. *J Allergy Clin Immunol* **111:**1153-1168.

Gottlieb AB, Griffiths CEM, Ho VC, Lahfa M, Mrowietz U, Murrell DF, Ortonne J-P, Todd G, Cherill R, Marks I, Emady-Azar S, and Paul CF (2005) Oral pimecrolimus in the treatment of moderate to severe chronic plaque-type psoriasis: a double-blind, multicentre, randomized, dose-finding trial. *Br J Dermatol* **152:**1219-1227.

Graham-Brown RAC and Grassberger M (2003) Pimecrolimus: a review of pre-clinical and clinical data. *Int J Clin Pract* **57:**319-327.

Grassberger M, Baumruker T, Enz A, Hiestand P, Hultsch T, Kalthoff F, Schuler W, Schulz M, Werner F-J, Winiski A, Wolff B, and Zenke G (1999) A novel anti-inflammatory drug, SDZ ASM 981, for the treatment of skin diseases: *in vitro* pharmacology. *Br J Dermatol* **141:**264-273.

Guengerich FP (1999) Cytochrome P-450 3A4: regulation and role in drug metabolism. *Annu Rev Pharmacol Toxicol* **39:**1-17.

Hughes P, Musser J, Conklin M, and Russo R (1992) The isolation, synthesis and characterization of an isomeric form of rapamycin. *Tetrahedron Lett* **33:**4739-4742.

Kronbach T, Mathys D, Umeno M, Gonzalez FJ, and Meyer UA (1989) Oxidation of midazolam and triazolam by human liver cytochrome P450IIIA4. *Mol Pharmacol* **36:**89-96.

Moenius T, Baumann K, Bulusu M, Schweitzer A, and Voges R (2001) Labeling of pharmacologically active macrocycles, in *Synthesis and applications of isotopically labeled compounds, vol. 7* (Pleiss U and Voges R eds) pp 424-429, John Wiley & Sons, Chichester.

Namiki Y, Kihara N, Koda S, Hane K, and Yasuda T (1993) Tautomeric phenomenon of a novel potent immunosuppressant (FK506) in solution: I. Isolation and structure determination of tautomeric compounds. *J Antibiot (Tokyo)* **46:**1149-1155.

Queille-Roussel C, Graeber M, Thurston M, Lachapelle JM, Decroix J, de Cuyper C, and Ortonne JP (2000) SDZ ASM 981 is the first non-steroid that suppresses established nickel contact dermatitis elicited by allergen challenge. *Contact Dermatitis* **42:**349-350.

Rappersberger K, Komar M, Ebelin M-E, Scott G, Burtin P, Greig G, Kehren J, Chibout S-D, Cordier A, Holter W, Richter L, Oberbauer R, Stuetz A, and Wolff K (2002) Pimecrolimus identifies a common genomic anti-inflammatory profile, is clinically highly effective in psoriasis and is well tolerated. *J Invest Dermatol* **119:**876-887.

Richmond CR, Langham WH, and Trujillo TT (1962) Comparative metabolism of tritiated water by mammals. *J Cell Comp Physiol* **59:**45-53.

Rigopoulos D, Ioannides D, Kalogeromitros D, Gregoriou S, and Katsambas A (2004) Pimecrolimus cream 1% vs. betamethasone 17-valerate 0.1% cream in the treatment of seborrheic dermatitis. A randomized open-label clinical trial. *Br J Dermatol* **151:**1071-1075.

Scheline RR (1973) Metabolism of foreign compounds by gastrointestinal microorganisms. *Pharmacol Rev* **25:** 451-523.

Scott G, Osborne SA, Greig G, Hartmann S, Ebelin M-E, Burtin P, Rappersberger K, Komar M, and Wolff K (2003) Pharmacokinetics of pimecrolimus, a novel nonsteroid anti-inflammatory drug, after single and multiple oral administration. *Clin Pharmacokinet* **42:**1305-1314.

Smith DA and Jones BC (1992) Speculations on the substrate structure-activity relationship (SSAR) of cytochrome P450 enzymes. *Biochem Pharmacol* **44:**2089-2098.

Smith RV (1978) Metabolism of drugs and other foreign compounds by intestinal microorganisms. *World Rev Nutr Diet* **29:**60-76.

Streit F, Christians U, Schiebel H-M, Meyer A, and Sewing K-F (1996) Structural identification of three metabolites and a degradation product of the macrolide immunosuppressant sirolimus (rapamycin) by electrospray-MS/MS after incubation with human liver microsomes. *Drug Metab Dispos* **24:**1272-1278.

Vidal C, Kirchner GI, and Sewing K-F (1998) Structural elucidation by electrospray mass spectrometry: an approach to the in vitro metabolism of the macrolide immunosuppressant SDZ RAD. *J Am Soc Mass Spectrom* **9:**1267-1274.

Wellington K and Noble N (2004) Pimecrolimus: A review of its use in atopic dermatitis. *Am J Clin Dermatol* **5:**479-495.

Wolff K, Caro I, Fleming C, Hanifin J, Papp K, Reitamo S, Rustin M, Shear N, Silny W, Korman N, and Paul C (2003) Treatment with oral pimecrolimus improves atopic eczema with a clear dose-response effect (conference abstract). *J Eur Acad Dermatol Venereol* **17(Suppl. 3):**182-183 (P2-38).

Zenke G, Strittmatter U, Fuchs S, Quesniaux VFJ, Brinkmann V, Schuler W, Zurini M, Enz A, Billich A, Sanglier J-J, and Fehr T (2001) Sanglifehrin A, a novel cyclophilin-binding compound showing immunosuppressive activity with a new mechanism of action. *J Immunol* **166:**7165-7171.

Zollinger M, Glaenzel U, Baldeck J-P (2002) Species comparison of the metabolism of pimecrolimus: a complex problem solved by LC-MS (conference abstract). Proceedings of the

50th ASMS Conference on Mass Spectrometry and Allied Topics, Orlando, Florida, June 2-6, 2002.

Footnotes.

Part of this work has been presented at the 50th ASMS Conference on Mass Spectrometry and Allied Topics, Orlando, FL, USA, June 2 - 6, 2002.

Address for reprint requests: Dr. Markus Zollinger, Novartis Pharma AG, WKL-135.2.21, P.O. box, CH-4002 Basel, Switzerland. E-mail: markus.zollinger@novartis.com

Legends for figures.

Fig. 1. Chemical structure of pimecrolimus (SDZ ASM 981). Positions of tritium labeling indicated by asterisks. In the *in vitro* blood distribution study [^{3}H]pimecrolimus was labeled in position 32. In all other studies [^{3}H]pimecrolimus was labeled in positions 5 and 6.

Fig. 2. Time-profiles of total radiolabeled components (radioactivity) and pimecrolimus in blood of four healthy male subjects treated with a single oral dose of 15 mg [^{3}H]pimecrolimus.

Fig. 3. Representative metabolite patterns *in vivo* (A-D) following a single oral dose of 15 mg [^{3}H]pimecrolimus administered to a healthy male subject and *in vitro* (E-H) after incubation of [^{3}H]pimecrolimus (1 µM initial concentration) with human liver microsomes (pool of ten individuals; 50 µg/ml microsomal protein).

Fig. 4. Electrospray mass spectrum of pimecrolimus (main tautomer) in the presence of lithium acetate, positive ion mode. Instrumental settings as described in *Materials and Methods*.

Fig. 5. Metabolite pattern of [^{3}H]pimecrolimus in an incubate with human liver microsomes. Initial substrate concentration 40 µM, pooled microsomes from ten individual livers, 4 mg microsomal protein/ml, 2 min incubation time. The information on the metabolite structures obtained by LC-MS is given in the form of metabolite names consisting of reaction codes, substructure codes and isomer numbers.

Reaction codes: D, *O*-demethylation; K, oxidative dechlorination; O, hydroxylation.

Substructure codes: x, reaction within substructure x; y, reaction within substructure y (see Fig. 4). Isomer numbers: numbering of isomers or tautomers (irrespective of substructure codes); discontinuous numbers due to additional isomers detected in incubates with animal liver microsomes (not shown).

Example 2DxxOx_7: two *O*-demethylations (2D), both in substructure x, in addition one hydroxylation (O) in substructure x, isomer (or tautomer) number 7.

Fig. 6. Overview of metabolic pathways and tautomerizations of [^{3}H]pimecrolimus in humans.

Fig. 7. Turnover of pimecrolimus by recombinant microsomes. [^{3}H]Pimecrolimus (1 µM initial substrate concentration) was incubated with microsomes prepared from recombinant human B-lymphoblastoid cell lines heterologously expressing human P450 isoenzymes. The amounts of recombinant P450 in the incubates (12.5, 21.5, 5.3, 19.4, 13.5, 12.3, 6.4, 8.3, 29.1, and 17.0 pmol of CYP1A2, CYP2A6, CYP2B6, CYP2C8, CYP2C9, CYP2C19, CYP2D6, CYP2E1, CYP3A4, and CYP4A11, respectively) were representative of the highest P450 concentration or marker activity found for the respective isoform in a panel of 12 individual human liver microsomes. Given are the amounts of [^{3}H]pimecrolimus metabolized during 20 min incubation time. Control: microsomes from recombinant cells containing P450 reductase only.

Table 1

Pharmacokinetic parameters of radioactivity (total radiolabeled components) and pimecrolimus in blood

Data obtained from healthy male subjects following a single oral dose of 15 mg [^{3}H]pimecrolimus; mean ± S.D. of n = 4 except where noted differently; ranges in parentheses.

	Radioactivity	Pimecrolimus
C_{max} (pmol/ml)	69.8 ± 11.0 (58.0 - 83.6)	50.9 ± 10.4 (40.5 - 62.2)
C_{max} (ng/ml)		41.2 ± 8.5 (32.8 - 50.4)
t_{max} (h)	median: 1 (1 - 2)	median: 1 (1 - 3)
$AUC_{0-\infty}$ (pmol·h/ml)	1079 ± 273 (698 - 1305) [a]	266 ± 53 (188 - 300) [b]
$AUC_{0-\infty}$ (ng·h/ml)		216 ± 43 (152 - 243) [b]
CL/f (l/h) [c]		72 ± 18 (62 - 99)
V_z/f (l) [c]		6700 ± 3800 (3200 - 11100)
$t_{1/2}$ (h)	145 (100 - 191) [d]	62 ± 27 (35 - 92) [e]

[a] $AUC_{0-240\ h} + C_{240\ h} \cdot t_{1/2} / \ln 2$

[b] $AUC_{0-120\ h} + C_{120\ h} \cdot t_{1/2} / \ln 2$

[c] Clearance (CL) and terminal volume of distribution (V_z), both referring to blood concentrations, divided by absolute bioavailability (f; unknown)

[d] Could be determined in two subjects only

[e] Derived from blood concentrations between 48 and 120 h

Table 2

AUCs of [^{3}H]pimecrolimus and its metabolites in blood

Healthy male subjects treated with a single oral dose of 15 mg [^{3}H]pimecrolimus. Data derived from metabolite patterns (examples in Fig. 3A and B); mean ± S.D. of n = 4.

	Radioactivity	Pimecrolimus	Metabolite Dx_1	Highly polar metabolites (front peak)	Sum of additional trace metabolites
$AUC_{0\text{-}24\ h}$ (pmol·h/ml)	387 ± 81	189 ± 50	18 ± 7	35 ± 8	144 ± 30
$AUC_{0\text{-}24\ h}$ (%)	100	49	5	9	37

DMD Fast Forward. Published on February 7, 2006 as DOI: 10.1124/dmd.105.007732
This article has not been copyedited and formatted. The final version may differ from this version.

Table 3

Cumulative excretion of radioactivity and pimecrolimus in urine and feces

Data from healthy male subjects following a single oral dose of 15 mg [^{3}H]pimecrolimus; mean ± S.D. of n = 4.

	Urinary excretion (% dose) [a]		Fecal excretion (% dose) [b]		Total excretion (% dose)
	Radioactivity	Pimecrolimus	Radioactivity	Pimecrolimus	Radioactivity
0-96 h	2.0 ± 0.4	not determined	71.9 ± 15.8	not determined	73.9 ± 15.3
0-168 h	2.3 ± 0.5	not detected	77.5 ± 13.7	0.7 ± 0.9	79.8 ± 13.2
0-240 h	2.5 ± 0.6	not determined	78.4 ± 13.8	not determined	80.9 ± 13.2

[a] Including tritiated water (0.5 ± 0.2% of dose in urine collected between 0 and 168 h)

[b] Not including tritiated water

Table 4

Distribution of [^{3}H]pimecrolimus between human plasma and blood cells in vitro *at 37°C*

Mean ± S.D. of n = 3 determinations using a pool of blood from three subjects; hematocrit 45 ± 1 %.

Blood concentration (ng/ml)	% in plasma
1	12.0 ± 0.4
34	12.5 ± 0.7
277	24.5 ± 6.0
556	49.6 ± 2.5
1016	70.5 ± 4.6

Table 5

Pharmacological activity of pimecrolimus metabolite pools

The measurements were performed by an IL-2 reporter gene assay. Metabolites were obtained from incubates of [^{3}H]pimecrolimus (10 µM initial concentration) with human liver microsomes (pool from ten individual livers; 1 mg microsomal protein/ml) for 5, 15 and 60 min. Metabolite pools were isolated by HPLC. The metabolites in Fraction 1 (highly polar metabolites) and Fraction 2 (moderately polar and nonpolar metabolites but no parent drug) eluted between 0 and approximately 10 min and between approximately 10 and 93 min, respectively, under the chromatographic conditions of the metabolite patterns (cf. Fig. 3).

	Incubation time [a]	Concentration-normalized pharmacological activity relative to that of pimecrolimus
Fraction 1	5 min	<3%
	15 min	<1%
	60 min	<0.3%
Fraction 2	5 min	9%
	15 min	4%
	60 min	0.5%

[a] Conversion of pimecrolimus to metabolites: 59% at 5 min, 84% at 15 min, 100% at 60 min

DMD Fast Forward. Published on February 7, 2006 as DOI: 10.1124/dmd.105.007732

Figure 1

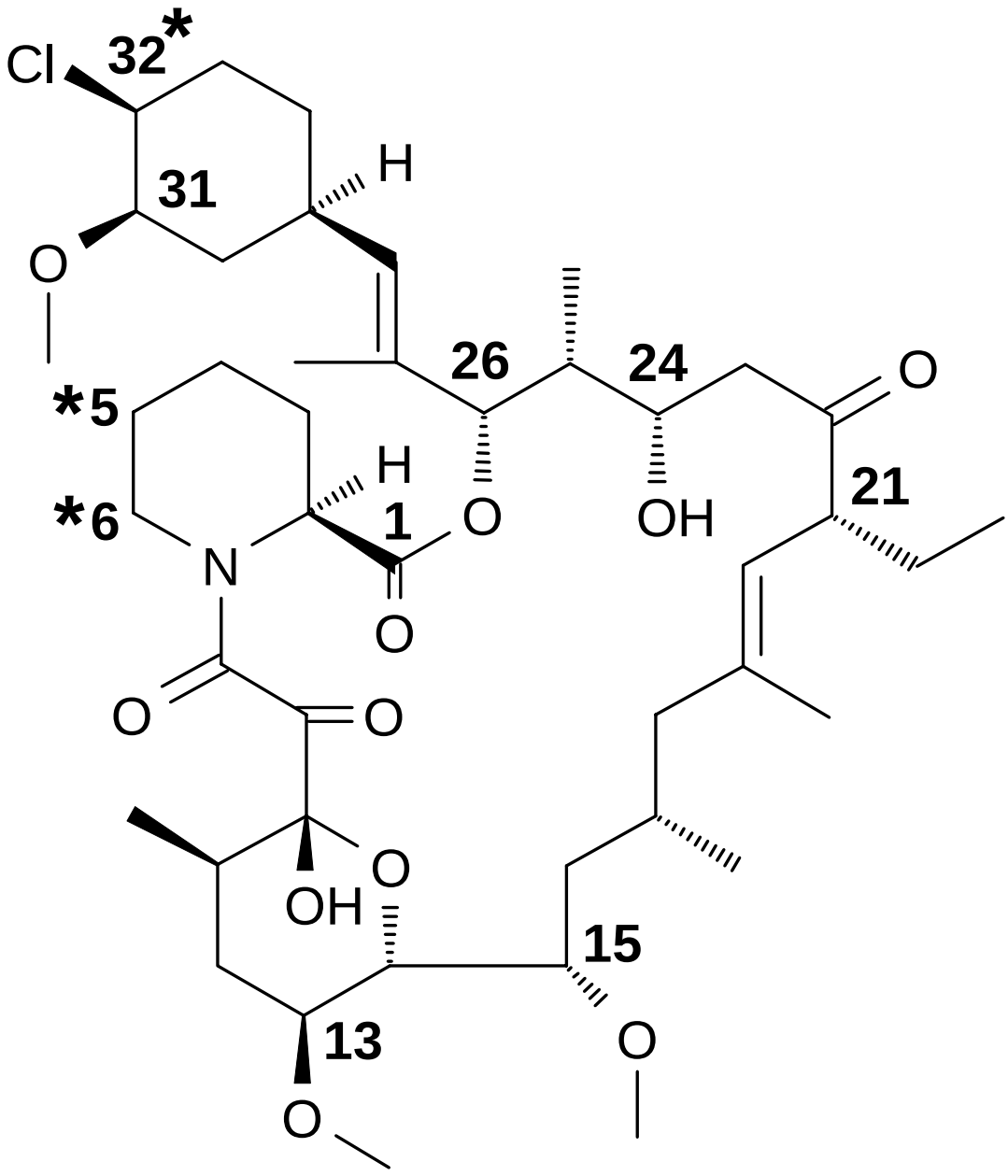

DMD Fast Forward. Published on February 7, 2006 as DOI: 10.1124/dmd.105.007732
This article has not been copyedited and formatted. The final version may differ from this version.

Figure 2

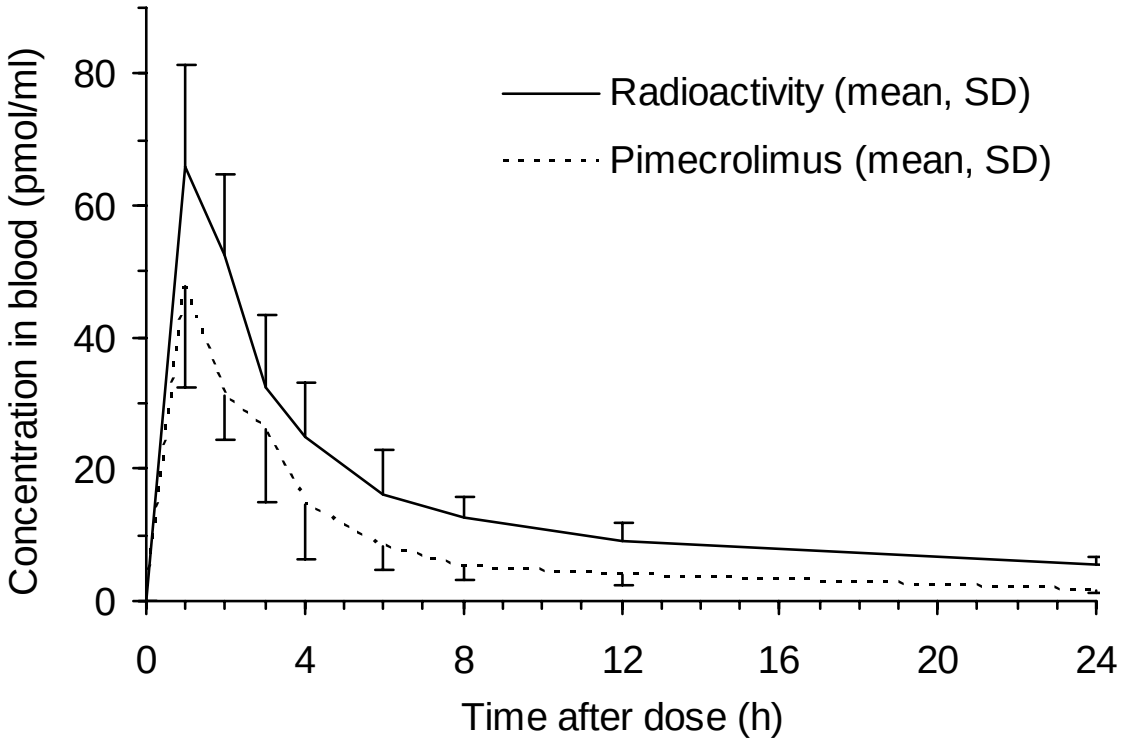

DMD Fast Forward. Published on February 7, 2006 as DOI: 10.1124/dmd.105.007732
This article has not been copyedited and formatted. The final version may differ from this version.

Figure 3

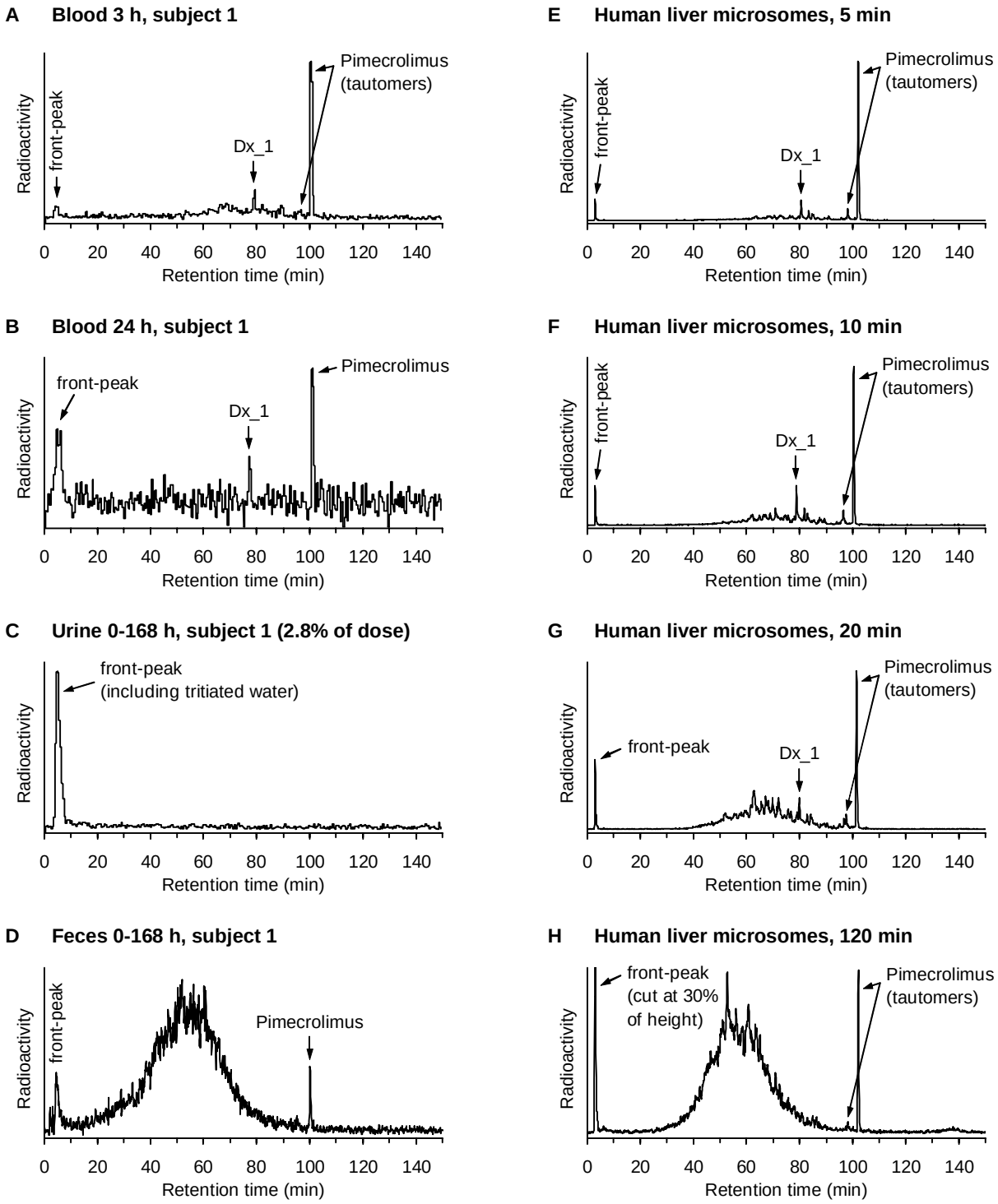

DMD Fast Forward. Published on February 7, 2006 as DOI: 10.1124/dmd.105.007732
This article has not been copyedited and formatted. The final version may differ from this version.

Figure 4

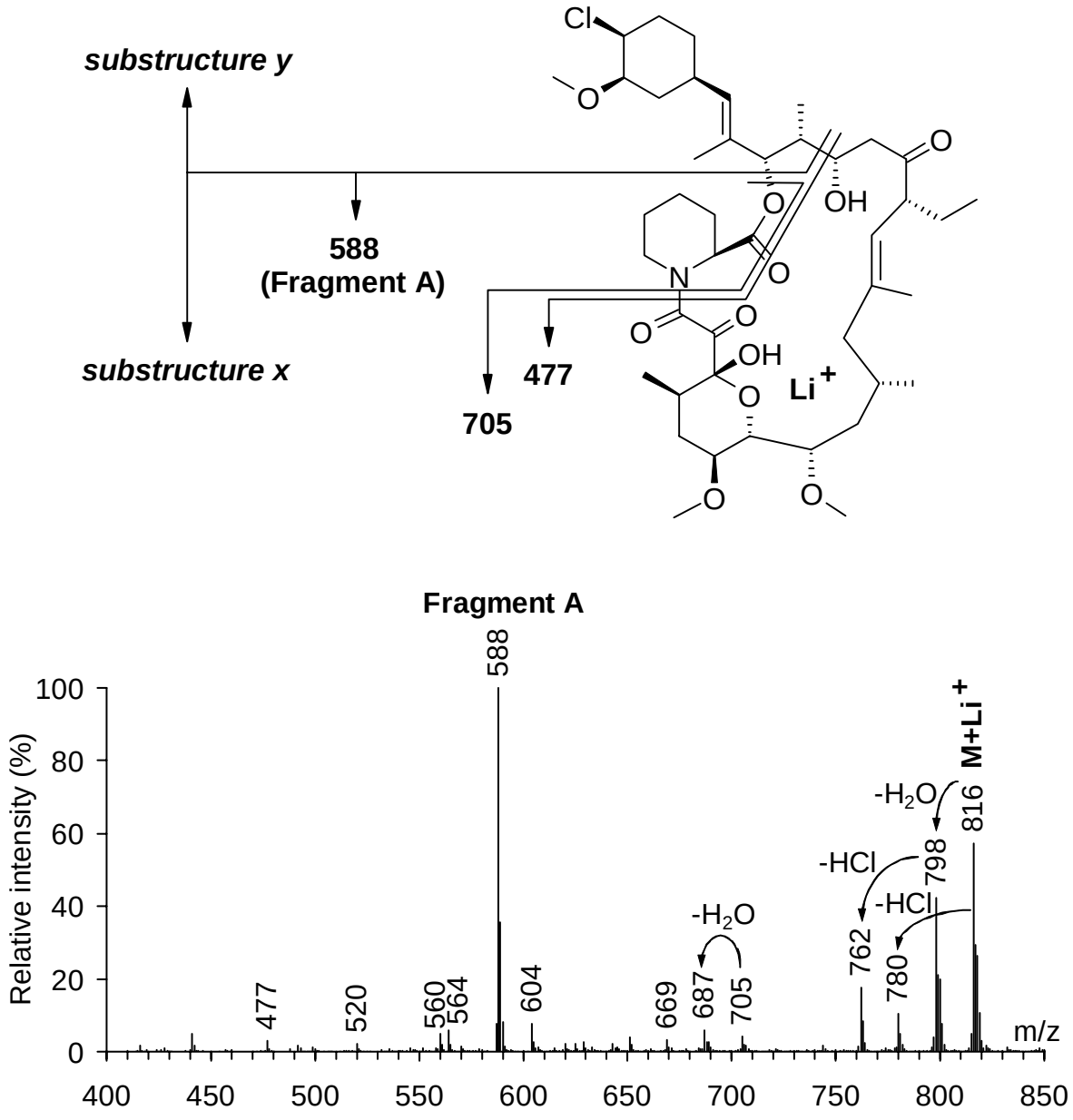

DMD Fast Forward. Published on February 7, 2006 as DOI: 10.1124/dmd.105.007732
This article has not been copyedited and formatted. The final version may differ from this version.

Figure 5

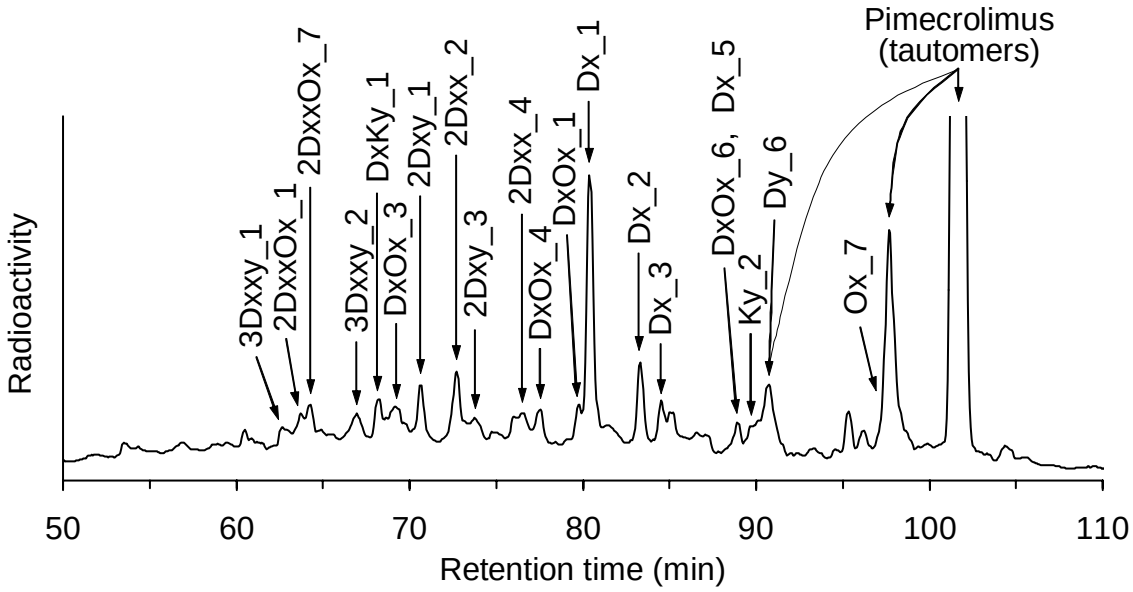

DMD Fast Forward. Published on February 7, 2006 as DOI: 10.1124/dmd.105.007732

Figure 6

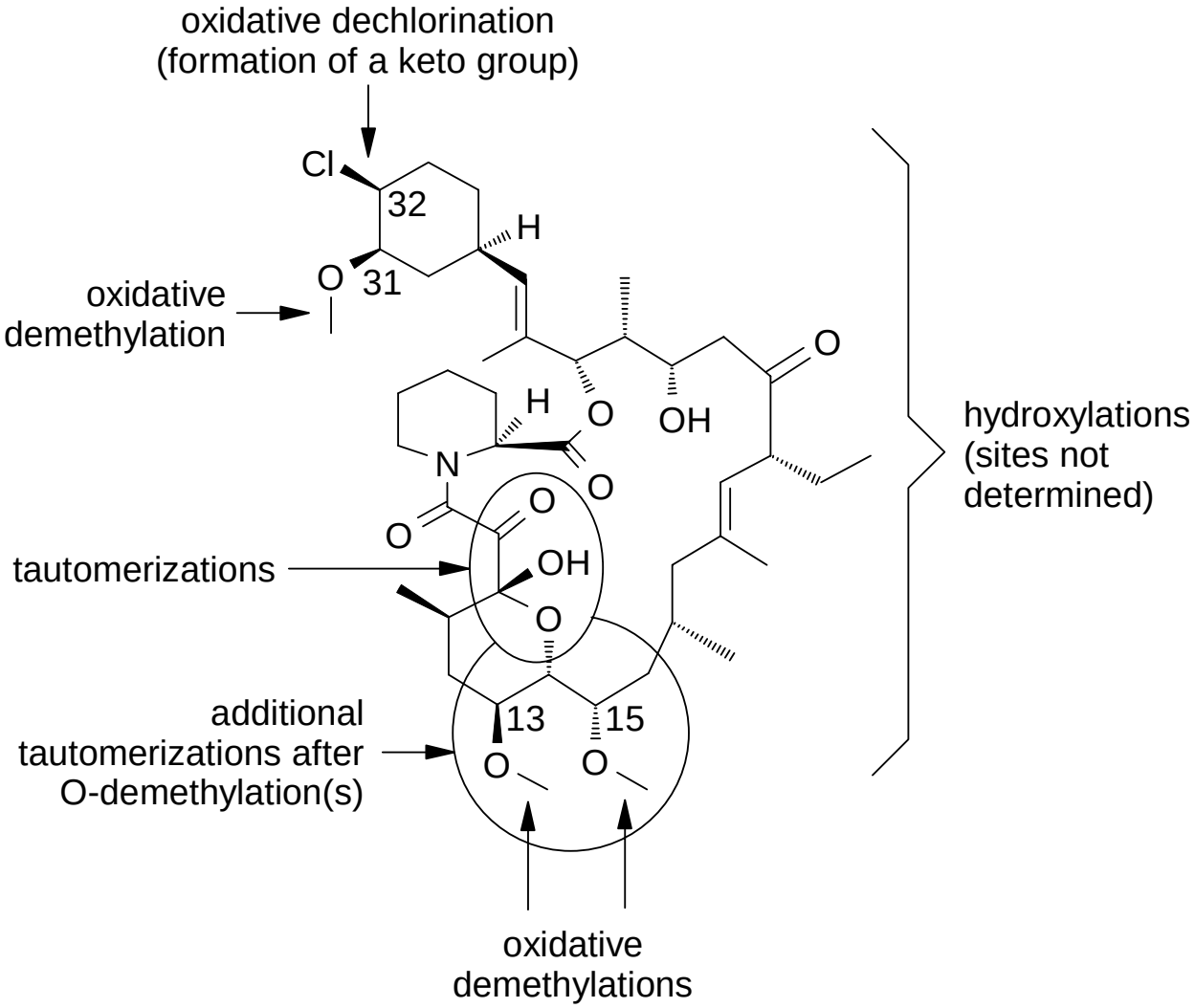

DMD Fast Forward. Published on February 7, 2006 as DOI: 10.1124/dmd.105.007732
This article has not been copyedited and formatted. The final version may differ from this version.

Figure 7